Visualizing flat spacetime: Viewing optical versus special relativistic effects

Don V. Black[a)]
Department of Electrical Engineering and Computer Science, University of California at Irvine, Irvine, California 92714

M. Gopi[b)]
Department of Information and Computer Sciences, University of California at Irvine, Irvine, California 92714

Frank Wessel[c)]
Department of Physics & Astronomy, University of California at Irvine, Irvine, California 92714

Renato Pajarola[d)]
Computer Science Department, University of Zürich, Zürich, Switzerland

Falko Kuester[e)]
California Institute for Telecommunications and Information Technology, University of California at San Diego, La Jolla, California 92093

(Received 20 August 2006; accepted 23 March 2007)

A visual representation of Minkowski spacetime appropriate for a student with a background in geometry and algebra is presented. Minkowski spacetime can be modeled with a Euclidean four-space to yield accurate visualizations as predicted by special relativity. The contributions of relativistic aberration as compared to classical prerelativistic aberration to the geometry are discussed in the context of its visual representation. © *2007 American Association of Physics Teachers.*
[DOI: 10.1119/1.2730838]

I. INTRODUCTION

This paper presents a Euclidean 4D model that can be used to view and explain Minkowski spacetime without resort to higher mathematics. The simple intuitive method presents the fundamental concepts underlying the theory of special relativity and enables teachers to lead students from Euclidean geometry into flat spacetime.

For simplicity, temporal homogeneity[1] and a flat[2] spacetime with no acceleration are assumed, and lighting effects are not considered. Under these conditions flat Minkowski spacetime is Euclidean for an inertial observer. The corresponding model can then be viewed and animated based on 4D raytracing.

Temporal extrusion of an inertial 3D object into 4-space along its normalized velocity 4-vector (worldline), followed by the Lorentz transformation (length contraction and time dilation) of the object into the inertial reference frame of the stationary camera are used to model object behavior. The camera can then be moved along the time axis, raytracing the 4D space, and creating an image collection that can subsequently be combined into a video sequence capturing the time-varying effects.[3]

In the following we will discuss our fundamental assumptions and the Minkowski 2D and 3D spacetime diagrams, describe our model and the construction of 4D objects from 3D objects, and demonstrate the resulting animations of 3D objects in 4D spacetime.

II. THEORY

As pointed out in Ref. 4 and demonstrated by Terrell[5] and Penrose,[6] the visual phenomena we explore here can be described as the combination of a nonrelativistic purely optical effect due to finite light speed that was discovered by Roemer in 1677,[7] and special relativity's four-dimensional spacetime introduced by Minkowski in 1908.[8] The finite speed of light leads to effects analogous to those of sound, as in the case of locating the position of a fast high flying jet by the sound of its engines. Finite and invariant light speed requires the physical phenomena predicted by special relativity: time dilation and length contraction. Time dilation is observable only if there is a variation in the object during the viewing period, as in the muon particle's decay. Length contraction is observable by differences between the geometry of a relativistic object at rest and in motion.

A. Background

Relativistic 4D spacetime (t,x,y,z) is often labeled $(3+1)$D, with three spatial dimensions (x,y,z) and one time dimension t. Similarly, a 3D spacetime (t,x,y) can be referred to as $(2+1)$D, with two spatial dimensions (x,y) and one time dimension t.

The most convenient units for our purposes are relativistic units where $c=1$. The benefit of using relativistic units is that the units along all the spacetime axes have the same scale, resulting in a lightray traveling one unit along the spatial axes for each unit it travels along the time axis. A lightray c can thus be represented in a Minkowski 2D spacetime diagram as a 45° bisector, or in a 3D spacetime diagram as the surface of a right circular cone, both shown in Fig. 1. We will use the light-second, the distance light travels in a second, as the basic unit of measure.

An object's worldline is its 4D path through spacetime. The instantaneous direction of an object's worldline is the object's proper time axis. The slope of this proper time axis in the Minkowski diagram represents the object's speed. The worldline through flat spacetime of an object with a constant velocity is a straight line. The normalized tangent to an object's worldline is the object's instantaneous velocity four-vector.

A 3D object can be created by extruding[9] a 2D object in a direction perpendicular to the 2D plane in which the object

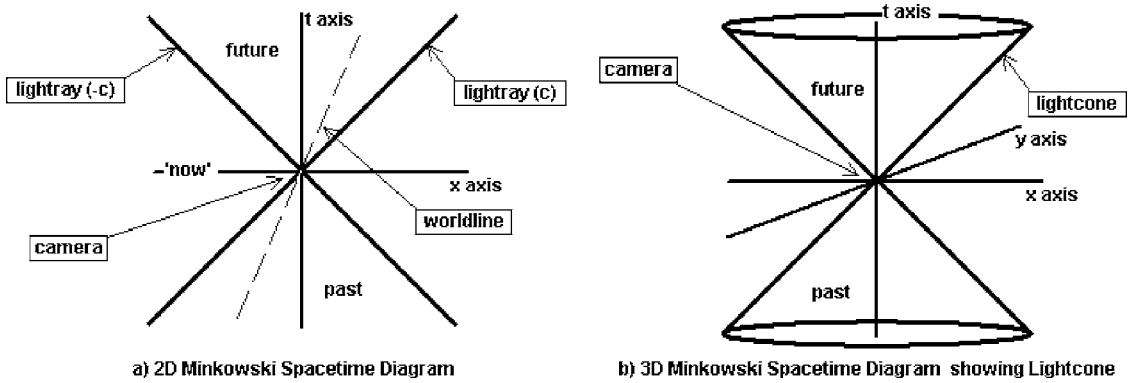

Fig. 1. (1+1)D and (2+1)D Minkowski spacetime diagrams. A camera at the origin can only "see" an event in the past whose lightray passes from that event through the camera at the origin.

lies [for example, by extruding a square from the (x,y) plane along the z axis]. Likewise, a 4D object can be created by extruding a 3D object in a direction orthogonal to the 3D hyperplane in which the object lies. A 4D example would be the extrusion of a cube from the (x,y,z) three-space, along the t axis. Two examples are shown in Figs. 2(a)–2(e). We call this temporal extrusion when a 3D object is extruded along its worldline.

Raytracing[10] is a geometric 3D image rendering procedure that colors a pixel on a viewplane by sending a ray from the viewpoint, through a pixel on the viewplane, and out into the scene's three-space where it may intersect the 2D surface element (such as a triangle) used to define the boundaries of a 3D object. The color of the object's surface at the intersection is used to color the corresponding pixel in the viewplane. This procedure is repeated for each of the pixels in the viewplane. Howard[11] adapted the open-source 3D raytracer POV-Ray[12] to relativistic raytracing by changing the angle of incidence as a lightray passes from one inertial reference frame to another. We found it necessary to increase the model's flexibility in order to demonstrate the difference between finite light speed effects and relativistic effects.

We have developed a simple four-dimensional raytracer by globally extending a 3D raytracer's[13] vector math from 3D to 4D and adding a fourth component t to the coordinate system. We constrain the lightrays to lie on the negative lightcone so that the ray travels through the model at light speed. The resulting 4D raytracer can image a Euclidean 4D space of 4D objects.

It can be shown that the length of an object with an arbitrary constant relativistic velocity[14] $\beta=v/c$ will contract in the direction of motion by a factor of $\gamma^{-1}=\sqrt{1-\beta^2}$. It can also be shown that the proper duration between any two events on the relativistic object's worldline will expand (dilate) by the Lorentz factor γ. These two phenomena are known as length contraction and time dilation, respectively.

B. Object construction

Any 3D object defined by bounding triangles such as the cube in Fig. 2(a) can be temporally extruded into a 4D hyperobject and inserted in the scene's four-space by extruding each f of its n individual triangles as follows. If we assume that the triangle's vertices are defined by their 3D coordinates in three-space, we insert a t component into each of the vertex coordinates and set t to some constant value, say t_0:

$$(x_i,y_i,z_i)_f \rightarrow (t_0,x_i,y_i,z_i)_f. \tag{1}$$

When performed on all three vertices i, the 2D triangle f will have a unique location in four-space.

The object now lies embedded in the xyz hyperplane that is orthogonal to the t axis at t_0 (*original object* in Fig. 3). Each of these triangles f, and hence the object composed from them, can be extruded into the fourth dimension by duplicating the vertices of the triangles with lesser (or greater) values for the t components. If the object is at rest in the camera frame, a constant Δt can be added to the t component of each of the object's original triangles in the t_0 hypersurface to create an f' duplicate triangle to be used as the object's position in the $t_0+\Delta t$ hypersurface:

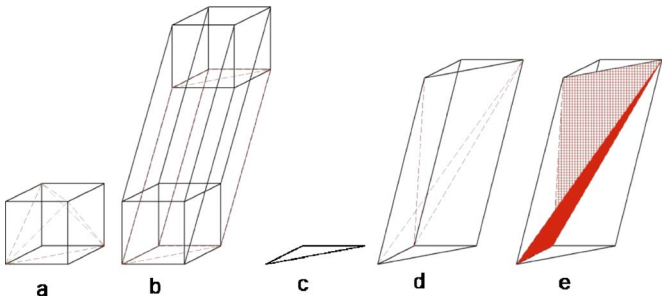

Fig. 2. Cube and triangle: extruded then tessellated.

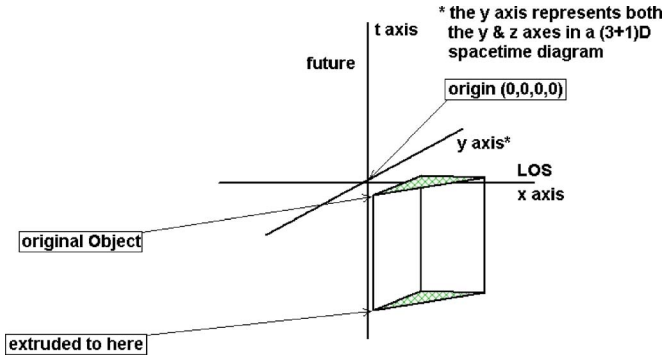

Fig. 3. Temporal extrusion: triangle at rest extruded into prism.

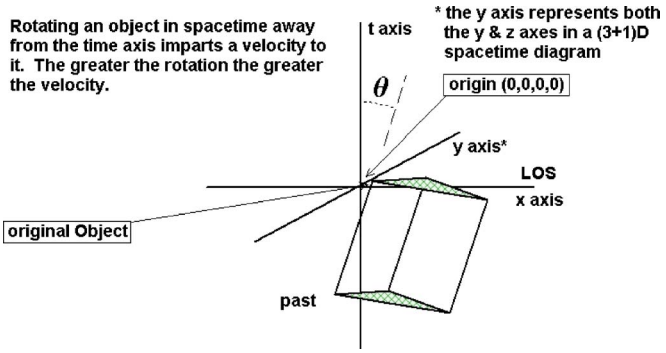

Fig. 4. Temporal extrusion not parallel to t axis. The object has moved with velocity$=\Delta x/\Delta t$.

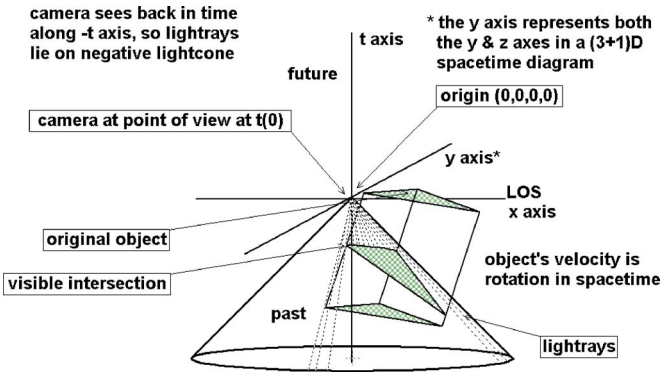

Fig. 5. Temporal extrusion of moving object with lightcone. A nonrelativistic spacetime: Finite light speed but no Lorentz transform.

$$(t_1,x_i,y_i,z_i)_{f'} = (t_0,x_i,y_i,z_i)_f + (\Delta t,0,0,0), \tag{2}$$

where $f=\{1,\ldots,n\}$ refers to each of the original triangles, $f'=n+\{1,\ldots,n\}$ to each of the corresponding extruded triangles, and $i=\{1,2,3\}$ to each of the corresponding vertices that define each triangle pair.

As shown in Fig. 3 where $\Delta t<0$, connecting the three vertices $[i=1,2,3$ in Eq. (2)] of the original triangle f with the respective vertices of the extruded triangle f' creates a 3D prism from the original triangle. Thus the triangle f exists only between t_0 and t_1, inclusive.

The prisms are then tessellated[15] into three adjacent tetrahedra as shown in Fig. 2(e). The 3D tetrahedra are necessary for the barycentric algorithm (described in the following) used to determine where the intersection with the lightray occurs on the three-manifold surface of the 4D object.

An object's velocity is represented by changing the position of the extruded end of the triangle (Fig. 4) with respect to the original end: $x_{\text{end}}=x_{\text{beg}}+\Delta x$ (spatial units). The speed in the camera frame would thus be $(\Delta x/\Delta t)\times$(spatial units)/(time units). Canceling the units yields the dimensionless fraction $\Delta x/\Delta t$. A lightray's slope $c=\pm 1$ is represented by both the diagonal lines and the surface of the lightcone of Fig. 1. For the general 3D case, where the distance traveled in time Δt is $\Delta d=\sqrt{\Delta x^2+\Delta y^2+\Delta z^2}$, the speed would be $\Delta d/\Delta t$, and Eq. (2) becomes

$$(t_1,x_i,y_i,z_i)_{f'} = (t_0,x_i,y_i,z_i)_f + (\Delta t,\Delta x,\Delta y,\Delta z). \tag{3}$$

C. Viewing 3D objects in (3+1)D spacetime

Consider a camera at the origin, whose line-of-sight (labeled LOS in Figs. 3–6) is collinear with the x axis. Because a lightray's worldline as depicted in the spacetime diagram lies on the lightcone, an object must cross the lightcone in the diagram in order to be visible to the camera. In fact, the object is visible to the camera only while it is intersecting that lightcone whose apex is coincident with the camera as shown in Fig. 5 (assuming the camera is pointing at the object).

Figure 5 depicts a right circular hypercone in four-space, whose symmetric axis is collinear with the $-t$ axis, and whose apex is coincident with the camera at the origin $(0,0,0,0)$. This hypercone's hypersurface, depicted by the inverted cone, has three dimensions, sufficient to contain the camera's focal point and the lightrays entering its lens. Although a three-manifold in four-space, this hypercone is known as a lightcone. A lightcone is thus the locus of all points that satisfy

$$(t_p,x_p,y_p,z_p) = \left(-\sqrt{x_p^2+y_p^2+z_p^2},x_p,y_p,z_p\right). \tag{4}$$

Note that the light travels from the object to the lightcone's apex at the origin. As depicted by the broken lines representing lightrays in Fig. 5, a camera located at the apex in this 4D model can see only those 3D objects whose extruded triangles (tetrahedra triads) intersect the lightcone. The only visible objects are those with vertex extrusion pairs (t_0,x_i,y_i,z_i) of the original object and (t_1,x_i,y_i,z_i) of its extruded end-cap, where

$$t_0 \geq \sqrt{x_i^2+y_i^2+z_i^2} \geq t_1, \quad \forall\,\{(t_0,x_i,y_i,z_i) \text{ and } (t_1,x_i,y_i,z_i)\}. \tag{5}$$

The intersecting portion of the extruded triangle is depicted by the triangle labeled *visible intersection* in Fig. 5. Note that geometric distortion in the object is caused by the intersection of the triangle and the lightcone. An object in the lightcone is easily detected because a straight line can be intersected with a 3D object in Euclidean four-space in the same manner as a straight line is intersected with a 2D object in three-space.

D. Animating spacetime objects

There is no mathematical or geometric limit to an object's speed in the model, its velocity being the slope of the temporal extrusion vector. For real physical objects, some physical mechanism must accelerate the object to the speed with which the object enters the model's laboratory inertial frame. We can assume that this speed must be less than that of light. The physical objects will then maintain an extrusion vector with a slope $|\Delta x|/\Delta t$ of less than 1, or an angle of less than 45° with respect to the t axis in the Minkowski diagram as shown by θ in Fig. 4. Because we are considering only uniformly moving objects, we can ignore the specifics of the spacetime rotation that yield the extrusion angle.[16]

Two classes of 4D objects have been implemented: one for the finite light speed objects and one for relativistic objects. The first is inserted into the scene without length contraction or time dilation as shown in Fig. 5, and the second is inserted with the Lorentz transformation as shown in Fig. 6. Conceptually, the former may be considered to have been measured in the laboratory inertial reference frame's units (it was al-

ready length contracted and time dilated), while in the latter case the object was measured in its own rest frame. The relativistic objects therefore must be length contracted and time dilated prior to insertion.

The animation procedure is straightforward. For example, to generate 20 s of animation at 10 frames per second ($\Delta t = 0.1$ s), the procedure is as follows.

(1) Beginning with the camera at (t_0, x_0, y_0, z_0), a view is rendered and saved.
(2) The camera is moved forward in time to (t_i, x_0, y_0, z_0), where $t_i = t_{i-1} + \Delta t$ and the view is rendered and saved.
(3) Repeat from step 2 while $t_i < 20$.

Notice that the camera's spatial components (x, y, z) do not change, only the time component of the camera position. Crucial to the simplicity of the procedure is the fact that the 4D object's bounding surfaces (and the tessellating tetrahedra that comprise those surfaces) do not change. The 4D world is static. Only the point of intersection of the lightcone changes as the camera and its lightcone progress along the t axis.

E. 4D intersection algorithm

Lightcone crossing events are detected by solving for the intersection of a lightray with each of an object's bounding tetrahedra. The set of lightrays is defined as that set of 4D straight lines passing from the camera through each of the pixels in the viewplane's pixel grid and out into 4D space. We use a 4D implementation of the barycentric algorithm to compute the intersections of the ray with all tetrahedra faces and select the intersecting event nearest to the camera (with the t value closest to 0). The array of 1D lightrays that originate from the gridded viewplane results in a 2D image of the objects projected onto that viewplane.

Because the objects have been Lorentz transformed prior to the intersection, such that their geometry is correct for the camera frame in which the intersection occurs, the geometric components of the lighting model, the surface normal and the reflection angle, can be used to approximate the pixel shade just as with a conventional lighting model in 3D rendering.

Photorealistic rendering requires the addition of lighting effects such as Doppler shift[17] and the searchlight effect, which could dominate the rendered image and obscure the visualization of the object's geometry.[18] For this reason, these effects were not implemented in our model.

III. RESULTS

Five consecutive frames of the video[3] generated with our software, extracted at 2 s intervals, are shown in Fig. 7(a)–7(e). Three models of relativistic motion are displayed in three panels in each image. The top panel shows the traditional ray-tracing technique, where the light speed is effectively infinite. In the middle panel, the nonrelativistic optical effects are shown, and in the bottom panel, the relativistic effects are displayed. The finite light speed camera (top panel) was moved ahead in time 18.675 s, an amount equal to the light speed delay from the center of the stage to the camera, so that the three panels of object pairs appear to be in approximately the same positions. The object displayed is a flange (angle bracket) 2 light-seconds wide by 2 light-seconds deep by 4 light-seconds tall. Its thickness is negligible (being constructed of four 2D triangles). There are two identical flanges, one on the left side and one on the right side of the centerline.[19]

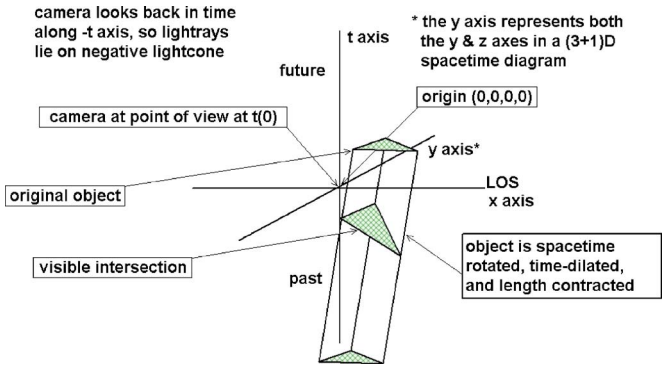

Fig. 6. A Lorentz transformed object. A velocity in the neighborhood of 86.6% of c yields a γ factor of around 2. The prism is shown length contracted by $\sim\frac{1}{2}$, and its proper time axis is dilated by ~ 2.

The scene is set on a stage with an overhead light source, both at rest in the camera frame. Two flanges approach, cross, and depart the centerline of the stage at 0.866 c. The geometric distortions of the center panel are due exclusively to classical aberration. Those of the bottom panel are due to the contributions of both classical and relativistic aberration.

The stage's mirrored backdrop shows the reflections of the flanges from behind. Note the difference in the positions of the reflections in the three models. The top panel shows the instantaneous reflections of the flanges, and the middle and bottom panels show the retarded reflections due to the light speed delay imposed by the added distance to be traveled by the lightray from the object to the mirror and back. The distances modeled are on the order of the size of the Jovian system.[20]

In Fig. 7(b) the bottom flanges appear to cross each other before the top flanges in Fig. 7(c). Note also in Fig. 7(e) that even with this head start, the top flanges arrive at their respective edges at the same time as the bottom flanges. The bottom flanges appear to approach faster in Fig. 7(b) and retreat slower in Fig. 7(d) than the top flanges, which is the visual evidence of the nonrelativistic optical effect known as classical aberration. The flanges approaching the centerline of the stage are obliquely approaching the camera. Aberration causes the angle from the centerline to the flanges to appear smaller than the proper angle of incidence, resulting in the object appearing closer to the centerline, or ahead of the object's proper position as depicted in the top view.

This aberration in the angle occurs for both the leading and the trailing edges of the flange, independently. As a result, the leading edge, which is closer to the centerline, appears to have moved further than the trailing edge, giving the impression of a wider flange. The opposite effect occurs as the flanges move away from the centerline. The flanges appear to incrementally speed up and simultaneously contract as they move relativistically away from the camera. These aberration effects are apparent in the bottom two panels of Fig. 7.

IV. CONCLUSIONS

We have visually demonstrated that implementing a simple algorithm that consists of a finite light speed compo-

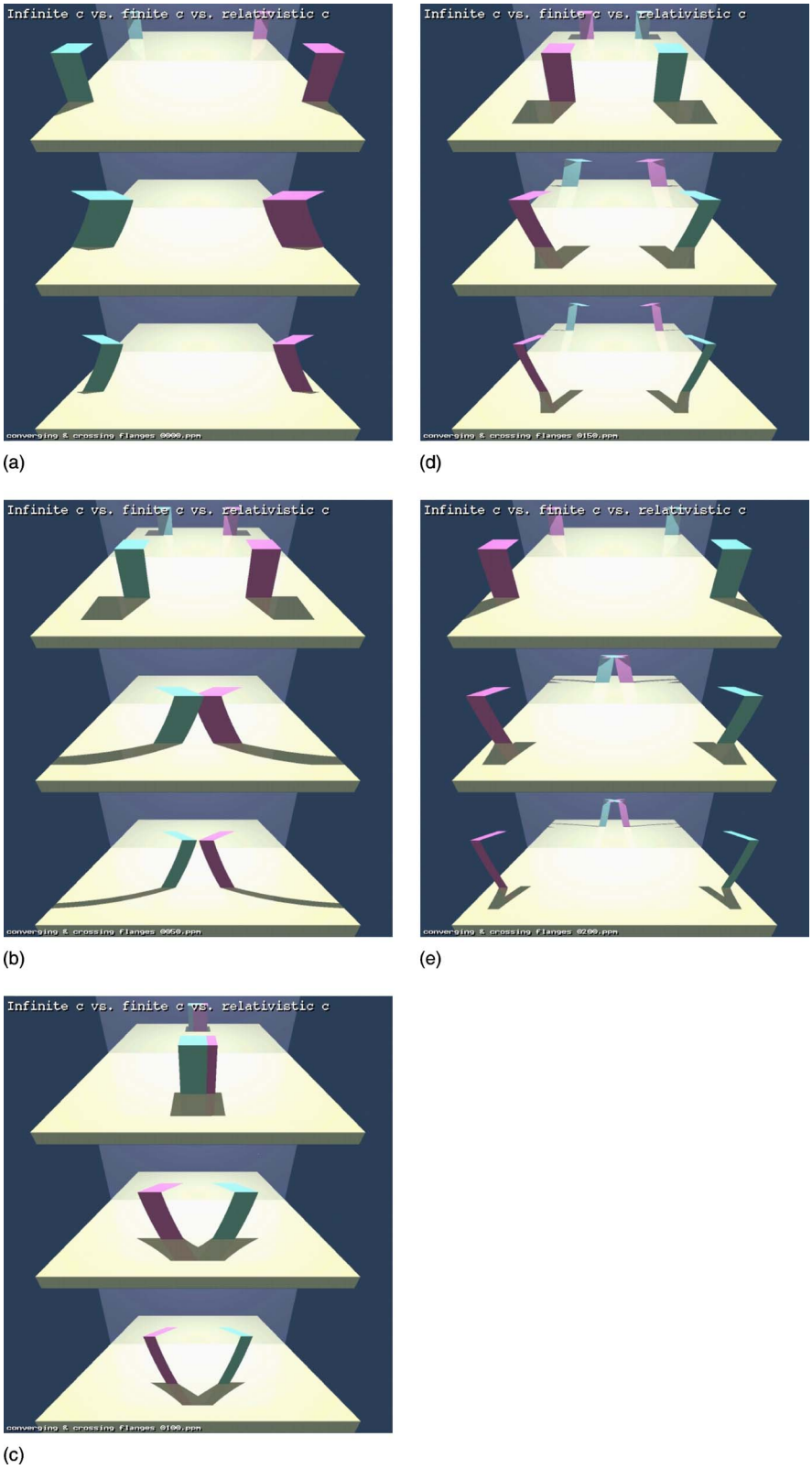

Fig. 7. (a) Sequential images of two 4D objects converging, and then crossing at 0.866 c on a mirrored background. Top panel: infinite light speed 4D raytracing. Center panel: prerelativistic spacetime. Bottom panel: relativistic spacetime. The top panel's nonrelativistic camera was moved ahead in time so that the flanges appear to be in the same positions as the bottom two panels' relativistic flange pairs. (b) The middle and bottom pairs of flanges appear to cross each other before those in the top panel. Classical abberation causes the approaching relativistic flanges to appear to move faster than their nonrelativistic counterparts. Classic abberation causes the approaching objects to appear wider than the nonrelativistic objects. This effect is offset by the relativistic length contraction as shown in the bottom panel. (c) The relativistic flanges in the bottom two panels appear to have crossed each other before those of the top panel. (d) The relativistic flanges appear to retreat slower than the nonrelativistic flanges. The relativistic flanges appear contracted in the direction of motion with respect to the nonrelativistic flanges due to the classical abberation. This effect is enhanced by the relativistic length contraction as shown in the bottom panel. (e) All three pairs of flanges appear to arrive at the edges at the same time. Their reflections follow them, retarded by the light's travel time from the objects to the mirror and back. It can be seen in the online color images that their reflections have not yet crossed one another.

nent and a length contraction component yields special relativistic visualizations similar to those using more complex visualization systems.[21] We have viewed the difference between nonrelativistic optical effects due to a finite light speed and those effects predicted by special relativity.

We have demonstrated that 3D animated sequences can be generated from a static 4D Euclidean spacetime, and that three-space can be visualized as the intersection of a light-cone and Euclidean four-space, where the slope of the light-cone's hypersurface determines the constant light speed in the model.

ACKNOWLEDGMENTS

We would like to thank Dr. Daniel Weiskopf and Dr. Arvind Rajaraman for their invaluable comments and suggestions. A special thanks also to Dr. James Arvo for his ToyTracer raytrace kernel code.

[a]Electronic mail: dblack@uci.edu
[b]Electronic mail: gopi@uci.edu
[c]Electronic mail: fwessel@uci.edu
[d]Electronic mail: pajarola@acm.org
[e]Electronic mail: fkuester@ucsd.edu

[1]Temporal homogeneity implies the object's visible elements do not change during the viewing period. Object shape, color, size, attitude, as well as velocity, are constant.

[2]Flat spacetime is not curved—objects obey Newton's laws, and a geodesic (straight line) is straight.

[3]See EPAPS Document No. E-AJPIAS-75-013706 for the video sequence, "Viewing classical and relativistic spacetime." This document can be reached via a direct link in the online article's HTML reference section or via the EPAPS homepage (http://www.aip.org/pubservs/epaps.html). The sequence is also available at ⟨www.hypervisualization.com/videos/black⟩.

[4]R. J. Deissler, "The appearance, apparent speed, and removal of optical effects for relativistically moving objects," Am. J. Phys. **73**, 663–669 (2005).

[5]J. Terrell, "Invisibility of the Lorentz contraction," Phys. Rev. **116**(4), 1041–1045 (1959).

[6]R. Penrose, "The apparent shape of a relativistically moving sphere," Proc. Cambridge Philos. Soc. **55**, 137–139 (1959).

[7]O. Roemer, "A demonstration concerning the speed of light," Philos. Trans. R. Soc. London **136**, 893–894 (1677).

[8]H. A. Lorentz, A. Einstein, H. Minkowski, and H. Weyl, *The Principle of Relativity* (Dover, New York, 1952), pp. 73–91.

[9]Extrusion is a computer aided design (CAD) construction operation that converts an n dimensional object into an $n+1$ dimensional object. The vertices, edges, and faces of the object are all extruded into the next higher dimension along the extrusion vector and then connected by edges, planes, and prisms, respectively.

[10]A. S. Glassner, *An Introduction to Ray Tracing* (Academic, San Diego, CA, 1989).

[11]A. Howard, S. Dance, and L. Kitchen, "Relativistic ray-tracing: Simulating the visual appearance of rapidly moving objects," Technical Report 95/21, The University of Melbourne, July 1995, pp. 1–13.

[12]POV-Ray, version 2.2, ⟨www.povray.org⟩.

[13]D. Kirk and J. Arvo, "*The ray tracing kernel*," in Proceedings of Ausgraph, edited by M. Gigante (ACM, Melbourne, Australia, 1988), pp. 75–82.

[14]Relativistic velocity is used to describe the relative speeds between two referents of 0.866 c or greater. The adjective relativistic also describes an object that is moving with relativistic velocity with respect to the camera frame in which the observer is at rest.

[15]Tessellated is used to describe a hyperplane (for example, a prism) tiled with a pattern (for example, a tetrahedra) in such a way as to leave no region uncovered. The covering hyper-tiles (tetrahedra) need be neither regular nor congruent.

[16]The temporal homogeneity assumption obviates the need for a discussion of hyperbolic rotation.

[17]P.-K. Hsiung, R. H. Thibadeau, C. B. Cox, R. H. P. Dunn, M. Wu, and P. A. Olbrich, "Wide-band relativistic doppler effect visualization," in *IEEE Visualization 1990 Proceedings* edited by A. E. Kaufman (IEEE Computer Society, Los Alamitos, CA, 1990), pp. 83–92.

[18]D. Weiskopf, U. Kraus, and H. Ruder, "Searchlight and doppler effects in the visualization of special relativity: A corrected derivation of the transformation of radiance," ACM Trans. Graphics **18**(3), 278–292 (1999).

[19]In the online version of this paper, the images are colored to show the left flange as blue and the right flange as pink.

[20]At the recorded animation rate (your playback may differ), the size of the stage is about 6 million Km on a side (20 light-seconds), easily large enough to encompass the planet Jupiter and the orbits of its four largest moons.

[21]D. Weiskopf *et al.*, "Visualization in the Einstein Year 2005: A case study on explanatory and illustrative visualization of relativity and astrophysics," in *IEEE Visualization 2005 Proceedings* (IEEE, New York, 2005), pp. 583–590.